

Biofabrication of Titanium Dioxide Nanoparticles Catalyzed by *Solanum surattense*: Characterization and Evaluation of their Antiepileptic and Cytotoxic Activities

Published as part of the ACS Omega virtual special issue "Phytochemistry".

Mohamed Mohany, Ihsan Ullah, Fozia Fozia,* Madeeha Aslam, Ijaz Ahmad,* Majid Sharifi-Rad, Salim S. Al-Rejaie, Nouf S. S. Zaghoul, Shakeel Ahmad, and Mourad A. M. Aboul-Soud



Cite This: *ACS Omega* 2023, 8, 16948–16955

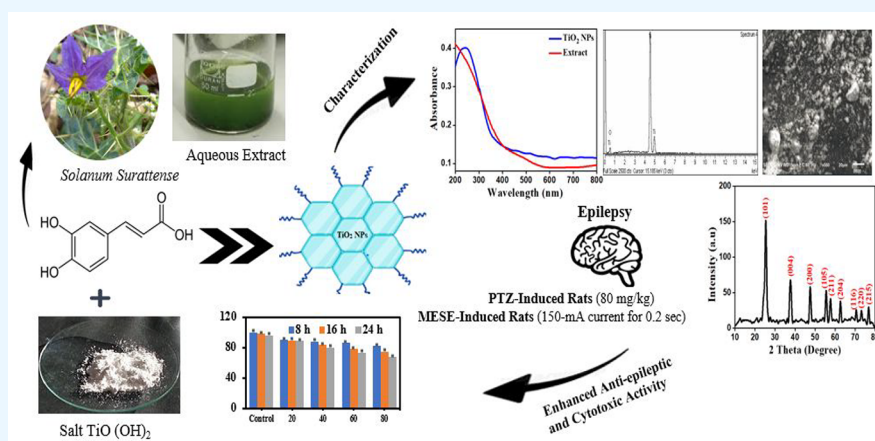


Read Online

ACCESS |

Metrics & More

Article Recommendations



ABSTRACT: The green synthesis of nanoparticles using plant extract is a new method that can be used in various biomedical applications. Therefore, the green approach was an aspect of ongoing research for the synthesis titanium dioxide nanoparticles (TiO₂ NP) using the *Solanum surattense* aqueous plant extract, which acts as a stabilizing and reducing agent. The synthesis of TiO₂ NPs was confirmed by energy dispersive X-ray (EDX), scanning electron microscopy (SEM), X-ray diffraction (XRD), Fourier transform infrared spectroscopy (FT-IR), and UV–visible spectroscopy (UV–vis) analyses. The excitation energy to synthesize TiO₂ NPs was identified through the UV–vis spectrophotometric analysis at a wavelength of 244 nm. Further, the FT-IR spectroscopy visualized different biomolecules like OH, C=O, C–H, and C–O that were present in an aqueous extract of the plant and were responsible for the stabilization of TiO₂ NPs. The crystallinity and phase purity of TiO₂ NPs were illustrated by the sharp peaks of the XRD pattern. The spherical morphology with sizes ranging from 10 to 80 nm was examined using SEM images. The elemental composition of TiO₂ NPs was revealed by the intensity and narrow widths of titanium and oxygen using EDX analysis. This report also explains the antiepileptic activity of TiO₂ NPs in a maximal electroshock-induced epileptic (MESE) and pentylenetetrazol (PTZ) model. The synthesized TiO₂ NPs showed maximum antiepileptic activity in the PTZ model, significantly decreasing the convulsions (65.0 ± 5.50 s) at 180 mg/kg in contrast to standard drug phenytoin, whereas the MESE model was characterized by the appearance of extensor, clonus, and flexion. The results showed that synthesized TiO₂ NPs significantly reduced the time spent in each stage (15.3 ± 0.20 , 16.8 ± 0.25 , and 20.5 ± 0.14 s) at 180 mg/kg as compared to control groups. Furthermore, the cytotoxicity of synthesized produced TiO₂ NPs demonstrated that concentrations ≤ 80 $\mu\text{g/mL}$ were biologically compatible.

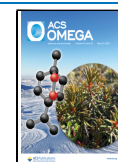
INTRODUCTION

In the past several years, metallic nanoparticles (NPs) have become prevalent in the field of nanotechnology. Metallic nanoparticles, such as platinum, silver, and gold, are renowned because of their positive effects on health.¹ Among various metal oxide nanoparticles, titania exists as oxide of titanium,

Received: February 10, 2023

Accepted: April 26, 2023

Published: May 8, 2023



recognized as TiO₂ NPs. Due to their versatile and respectable assets derived from their optical, physical, chemical, and electrical stability, TiO₂ NPs are the most frequently formed metal oxide nanoparticles.² TiO₂ NPs are prominent semiconductor nanoparticle with a bandgap energy of 3.0 eV for the rutile phase and that of 3.2 eV for the anatase phase; nevertheless, it remains difficult to find the brookite phase. The tetragonal crystal structure of TiO₂ NPs is easily accessible for anatase and rutile phases, while the brookite phase has an orthorhombic arrangement.³ Their physicochemical characteristics, such as the greater refractive index and ultraviolet (UV) light absorption capacity, of TiO₂ NPs make them useful in various fields.^{4–7} For instance, the cytotoxicity, gene expression, and the metabolic activities of TiO₂ NPs on human cell lines have induced inflammatory responses due to their thin film, transparency, relatively low cost, and chemical stability.⁸ TiO₂ NPs were employed as a cancer photothermal therapy (PTT), and they were further used for nonradiative recombination.⁹ Recently, TiO₂ NPs have gained a lot of attention for the treatment of pathogenic microorganisms that have made significant contributions to the development of antimicrobial agents.¹⁰ The pharmaceuticals are emerging pollutants that are increasingly being found in water systems. They have been detrimental to human and animal health. Using sophisticated metal oxide nanoparticles in a photocatalytic technique, the pharmaceutical medicines are removed from water.^{11,12} Different methods are used to synthesize TiO₂ NPs, e.g., chemical, physical, and green synthesis methods.^{13–15} The physical and chemical methods used toxic substances that are hazardous to the environment, as well as high pressure and temperature, and require sufficient space to set up the reaction conditions. Thus, the synthesis of TiO₂ NPs using the biological method has gained more attention because it does not require expensive equipment, high temperatures, and toxic chemicals. Therefore, different plant extracts were used to synthesize TiO₂ NPs, including *Luffa acutangula*,¹⁰ *Acorus calamus*,¹⁶ and *Pulicaria undulata*,¹⁷ which serve as reducing and stabilizing agents.

The World Health Organization (WHO) recognizes the major public health concern of epilepsy, which is activated by an imbalance between excitation and inhibition or hyperexcitability. Epilepsy is a prevalent neurological disease, with an estimated 50 million people suffering worldwide. The degree of effectiveness is influenced by the distinctive region, the types of seizures, and the region experiencing abnormal neuronal activity. Epileptic patients experience societal misconceptions, discrimination, social stigma, and negative attitudes that might discourage them from accessing care and being self-assured.¹⁸ Several antiepileptic drugs have been used to treat epilepsy, but the side effects exhibited by these drugs are of great concern. In addition, the mortality of epilepsy is increasing day by day; hence, the use of plant-based drugs for the treatment of epilepsy has drawn more attention. Several plants and their active ingredients have been studied in laboratory and clinical settings to determine the action of molecular mechanisms.^{19,20} Thus, it is essential to use a new antiepileptic drug with enhanced reliability and effectiveness. Therefore, the purpose of the current study was to synthesize TiO₂ NPs that are not reported in literature using plant extract of *Solanum surattense*, and in this article we are reporting a new source green method for the synthesis of TiO₂ NPs. Furthermore, extensive survey of the literature revealed that synthesized TiO₂ NPs have never been reported for the antiepileptic and cytotoxic activities. Herein, in this article we are reporting the green synthesis of TiO₂ NPs using

the plant extract of *Solanum surattense* and its biomedical applications for the first time.

Solanum surattense is a long-lasting medicinal plant belongs to the family Solanaceae and is used in folk and traditional medicine. The anti-inflammation and antiasthmatic activities show the efficient therapeutic potential of the *Solanum surattense* plant.²¹ The use of traditional drugs on a theoretical basis is a useful approach for modern development in the medical fields. Therefore, the goal of the current study was to shed light on previously unreported pharmacological actions of TiO₂ NPs using the *Solanum surattense* plant extract. All parts of the plant including stem, leaf, fruits, flowers, and roots have important phytoconstituents, including flavonoids, alkaloids (caffeic acid, coumarins, and triterpenoids), phenols, saponins, glycosides (solanosine), and steroids (campesterol, carpesterol, stigmastanol, daucosterol, cholesterol, and cycloortanol), that primarily act as capping and reducing agents for the synthesis of TiO₂ NPs.²² Moreover, the geometry, elemental composition, optical, and morphological properties of synthesized TiO₂ NPs were investigated by various techniques, including SEM, EDX, FT-IR, XRD, and UV–vis spectrophotometry. Thereis, this work was carried out to synthesize TiO₂ NPs using *Solanum surattense* aqueous plant extract and then to explore the antiepileptic activity. Furthermore, the cytotoxicity activity of the synthesized TiO₂ NPs is examined by using the MTT assay to determine their biocompatibility for biomedical applications.

■ MATERIALS AND METHODS

Preparation of Plant Extract. The whole plant of *Solanum surattense* was collected from Kohat, Khyber-Pakhtunkhwa, Pakistan. The plant was thoroughly cleaned with distilled water to get rid of any dust. Then, it was finely cut into very small pieces and dried in the shade at room temperature. About 20 g of the finely cut plant was taken and then immersed in 100 mL of distilled water, and the mixture was heated for 40 min. Further, the acquired plant extract was allowed to cool at room temperature before being filtered through Whatman Filter Paper no. 1 and kept refrigerated for the synthesis of TiO₂ NPs.

Green Synthesis of TiO₂ NPs. The synthesis of titanium dioxide nanoparticles was achieved by adding 20 mL of an aqueous plant extract of *Solanum surattense* into 80 mL of a 0.01 M solution of TiO(OH)₂ under stirred conditions in the rotatory orbital shaker at 200 rpm for 24 h at room temperature. The formation of nanoparticles takes place after constant stirring, which is demonstrated by the color transition of a solution from light green to whitish brown. The synthesized TiO₂ NPs were collected from the reaction mixture by centrifuging the solution for 20 min at 4000 rpm. The TiO₂ NPs were washed with distilled water and methanol two or three times to remove any trace of the unbound phytoconstituents. The isolated TiO₂ NPs were examined for other analysis.²³

Characterization of TiO₂ NPs. The titanium dioxide nanoparticles were then subjected to characterization using various insightful measurement techniques, including EDX, SEM, XRD, FT-IR, and UV–vis spectrophotometry.

UV–vis Spectroscopy. The capacity of a sample to absorb and disperse light is measured using UV–visible (UV–vis) spectroscopy. A light source and a focus lens were placed in front of the integrated TiO₂ NP solution, and the amount of light absorbed at wavelengths between 200 and 800 nm was calculated using a Shimadzu 3600 spectrometer. Due to the correlation between the absorption bands and the diameter aspect ratio of metal nanoparticles, UV–vis spectroscopy is the

most frequently used method confirm the formation of nanoparticles as well as to characterize their optical characteristics and electronic structure.

FT-IR Analysis. Fourier transform infrared (FT-IR) spectroscopy was used to identify the functional groups and the binding characteristics of titanium oxide nanoparticles. Simple wafers containing the titanium dioxide nanoparticles to be separated and KBr were used in the infrared spectrometer (JASCO-4600). The spectra of the sample were recorded at wavenumber ranges between 4000 and 500 cm^{-1} with a resolution of 4 cm^{-1} .

XRD Analysis. To determine the crystallinity and phase formation of TiO_2 NPs, an analytical technique called X-ray diffraction (XRD) is used. A nickel-filtered $\text{Cu K}\alpha$ radiation source ($6k = 1.54056$) was used for the X-ray diffractometer's XRD analysis. The instrument was operated at 30 mA and 40 kV while equipped with a graphite monochromator. The diffractogram was obtained in the 2θ range of 10–80°. The acquired raw data were analyzed using Origin software and compared to the common JCPDS database cards nos. 21-1276. (rutile) and 21-1272 (anatase).

SEM Analysis. Scanning electron microscopy was used to examine the morphological characteristics of the synthesized TiO_2 NPs. The dry TiO_2 NPs were then crushed into a powder. At that point, thin films of 10 mg of the TiO_2 NPs were applied to copper grids that had been coated with carbon after being redispersed in ethanol. With the help of finder helper electrons, SEM micrographs were formed at various magnifications with a working distance set to about 3 mm and an acceleration voltage of 5 eV.

Energy Dispersive X-ray (EDX). An energy dispersive spectroscopy (EDX) was employed to determine the surface shapes and elemental compositions of the synthesized TiO_2 NPs at an accelerating voltage of 20 keV.

■ ANTIPILEPTIC ACTIVITY

Animals. Female Wistar rats weighing between 150 and 200 g were used in experiments. They were kept in polypropylene cages in accordance with CPCSEA guidelines for the care and use of laboratory animals.

In Vitro Antiepileptic Assay. To investigate the antiepileptic activity, Wistar rats were collected from the animal house of the institute. Four groups of five Wistar rats each comprised 20 animals. Group 1 received 2 mL/kg, 10% *v/v* Tween 80; group 2 received phenytoin (25 mg/kg); and 80 and 160 mg/kg of TiO_2 NPs was given to groups 3 and 4, respectively. After 1 h, all groups in the pentylenetetrazol (PTZ) model received a PTZ injection (80 mg/kg). By placing each rat in a plexiglass box, the subsequent stages of seizures were observed for 60 min. Stage 0 is no response; stage 1 is twitching of the ear and face; stage 2 is for myoclonic jerks; stage 3 is convulsion by clonic forelimb; stage 4 is seizures through generalized clonic; and stage 5 is seizures via generalized tonic clonic or death within 60 min. In contrast, in the maximal electroshock induced epileptic (MESE) model, each rat received a unique electroshock after 1 h using ear-clip electrodes. With a 150 mA current frequency, the duration of the stimulus was 0.2 s. Afterward, clonic convulsions, tonic extensor phase, and tonic flexion were observed at different phases of analyses. The time the animals spent in each stage was noted.²⁴

Cytotoxic Activity of TiO_2 NPs. Cell Culture. The THP-1 cell line was cultured in RPMI-1640 medium containing 2 mM L-glutamine, 4.5 g/L glucose, and 10% fetal bovine serum. The

culture of the cell was preserved between 1×10^6 cells at 37 °C and 5% CO_2 and was regularly subcultured using a fresh medium, with fluid renewal carried out every two or three days.

MTT Assay. The cells under investigation were grown in culture flasks in an incubator with humidity control at 37 °C and 5% CO_2 . Following the expected level of THP-1 cell growth, the suspension of cells was rotated at 2000 rpm for 5 min, and the cell pellets were then resuspended in fresh RPMI-1640 medium. The count of the cell suspension was then altered to 1×10^6 cells/mL. Different TiO_2 NP concentrations (20, 40, 60, and 80 $\mu\text{g/mL}$) were added to the 96-well plate for the MTT (3-(4, 5-dimethyl-2-thiazol)-2,5-diphenyl-2H-tetrazolium bromide) assay. The treated cells were incubated with 5% CO_2 at 37 °C. The cell viability was assessed using the MTT assay after overnight incubation. Each well containing the sample received an addition of MTT (5 mg/mL) and was then left alone for 4 h. The formazan crystals were able to dissolve after being added to dimethyl sulfoxide (DMSO). We used a multimode reader to take absorbance readings at 570 nm (Biorad 680, USA). The relative absorbance of the number of dead and live cells in the sample was used to estimate the cell viability percentage.²⁵ The ratio of optical density (OD) between the control (cells without nanoparticles) and that of cells treated with various concentrations of nanoparticles was measured by the cell viability equation shown in eq 1.

$$\text{Cell Viability (\%)} = \frac{\text{OD Test}}{\text{OD Control}} \times 100\% \quad (1)$$

■ RESULTS AND DISCUSSION

UV–vis Analysis of TiO_2 NPs. The absorption spectra acquired from UV–vis spectroscopy displays the light absorption and the optical property characteristics of green synthesized TiO_2 NPs. The visual identification was made by the color change during the incubation of *Solanum surattense* plant extract with the titanium precursor solution. The color of the $\text{TiO}(\text{OH})_2$ precursor reaction with *Solanum surattense* extract changed to light green during the stirred incubation period.²⁶ The excitation of the surface plasmon resonance during the synthesis of TiO_2 NPs was the cause of this distinctive color variation. This is due to the abundant phytochemicals found in plant extracts, which act as capping agents and aid in the reduction of TiO_2 NPs. In light, the wave resonance of metal nanoparticles, especially TiO_2 NPs, coupled with the oscillation of electrons produces a free electron to absorb the surface plasmon resonance phenomenon. In contrast, the pure $\text{TiO}(\text{OH})_2$ solution without an aqueous plant extract did not show any absorption peak, as shown in Figure 1. When the plant extract solution was exposed to the TiO_2 precursor, the absorption spectra of the TiO_2 NPs formed in the solution showed absorbance peaks at about 244 nm, which are consistent with those of prior works.²⁷

FT-IR Analysis of TiO_2 NPs. The reduction of TiO_2 NPs was investigated using the FT-IR technique and was identified by the presence of functional groups. The KBr palletization technique was used to record the results within the range of 4000–500 cm^{-1} at a resolution of 2 cm^{-1} . The interaction of specific functional groups in the reduction and stabilization of TiO_2 NP formation was revealed by the FT-IR spectra of TiO_2 NPs and the plant extract from *Solanum surattense*, which showed band intensities in various regions. The prominent peaks observed in the plant extract were 3267, 1720, 1338, and 1149 cm^{-1} as mentioned in Figure 2. The peak at 3267 cm^{-1} was mainly due to

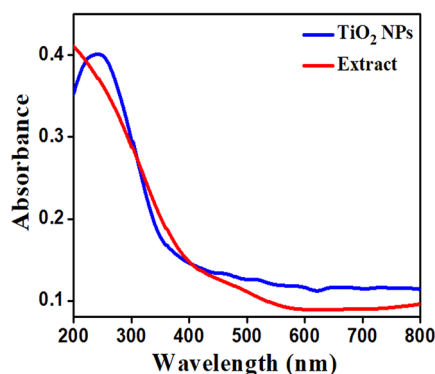


Figure 1. UV–visible spectra of synthesized TiO₂ NPs.

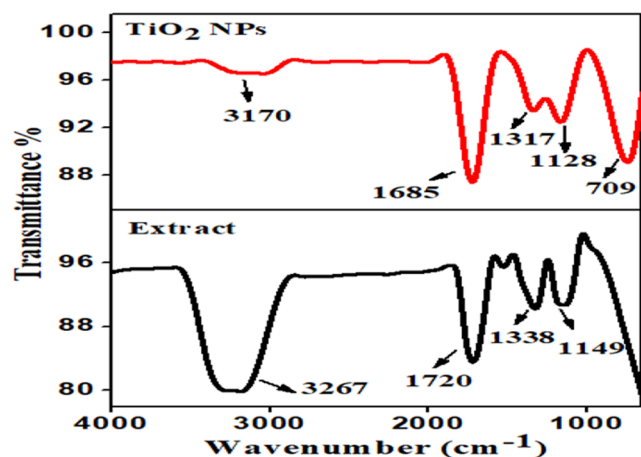


Figure 2. FT-IR spectrum of synthesized TiO₂ NPs and an aqueous plant extract *Solanum surattense*.

the stretching vibration of the OH groups in alcohol and phenol. The peak at 1720 cm⁻¹ correspond to the C=O group of carboxylic acid. The band at 1338 cm⁻¹ was assigned to the C–H stretching vibration of the alkyne group, while the peak at 1149 cm⁻¹ was attributed to bending vibration of the C–O group.²⁸ The functional groups present in the *Solanum surattense* plant extract, such as OH, C=O, C–H, and C–O, may have been obtained from flavonoids, carboxylic compounds, aromatic amine groups, and secondary alcohols and serve as capping agents for the formation of TiO₂ NPs.²⁹ The bands shift to 3170, 1685, 1317, and 1128 cm⁻¹ after the reduction of the titanium ion into TiO₂ NPs, whereas the peculiar signal at 450–800 cm⁻¹ was caused by the vibration of the Ti–O–Ti bond for TiO₂ nanoparticles.³⁰ Therefore, we concluded that TiO₂ NPs were capped and stabilized by different biomolecules present in the plant extract.

XRD Pattern of TiO₂ NPs. The phase purity and crystalline nature of TiO₂ NPs synthesized using *Solanum surattense* plant extract were determined by the XRD technique. The resulting diffractogram for TiO₂ NPs confirms the strong crystalline nature of the TiO₂ NPs that were obtained due to sharp intense peaks with narrow widths. The estimations of Bragg reflections at 2θ could determine the orientation of nanoparticles. Figure 3 shows the diffraction angles of 25.34°, 37.60°, 47.00°, 55.23°, 62.01°, 70.32°, and 76.33°, which were attributed to (101), (004), (200), (105), (211), (204), (116), (220), and (215), respectively. The XRD results demonstrate the formation of well-crystalline titanium with an anatase phase, which is fully

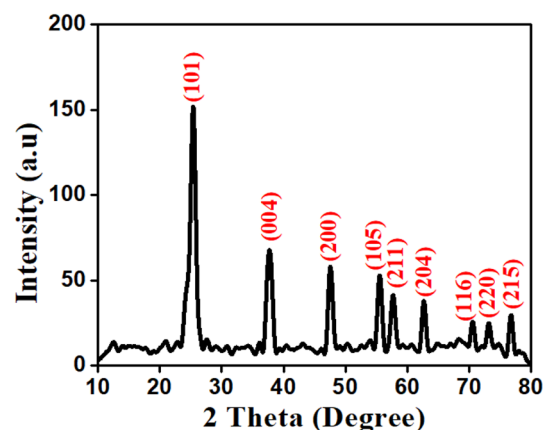


Figure 3. XRD patterns of synthesized TiO₂ NPs.

evident in the standard database of JCPDS (#21-1272).³¹ The exclusion of any other characteristic peaks indicated the absence of impurities in the obtained TiO₂ NPs, and the precursor was totally transformed into a product. Therefore, the resultant XRD pattern revealed the phase purity of the resultant TiO₂ NPs, indicating that the extract has the reduction potential to synthesize highly crystalline nanoparticles without any amorphous nature. The crystallographic plane was associated with the apparent diffraction angle at 25.34° of the (101) plane of the TiO₂ anatase phase. The average diameter of particle was determined by using Scherrer's equation as shown in eq 2.

$$6D = \frac{0.9\lambda}{\beta \cos \theta} \quad (2)$$

Here the wavelength of the X-ray is represented by λ, diffraction angles correspond to θ, and the fwhm in radians is denoted by β. The average crystallite size was determined from the diffraction measurements to be approximately 19.69 nm.

SEM Analysis of TiO₂ NPs. Using a scanning electron microscope, the surface morphology and size of synthetic nanoparticles were assessed. It was noted from the SEM images that the particles are evenly distributed across the surface. The synthesized nanoparticles are spherical in shape and are clustered together in bunches (Figure 4). The size of the nanoparticles was observed to be in the range of 10–80 nm. The average crystalline size determined by XRD and the particle size discovered by SEM have a strong correlation. In general, the relationship between the nanoparticle surface volume and the

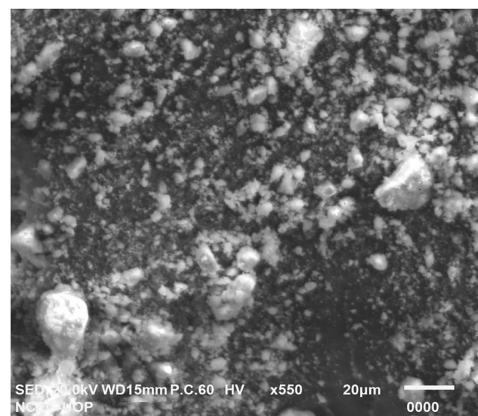


Figure 4. SEM images of synthesized TiO₂ NPs.

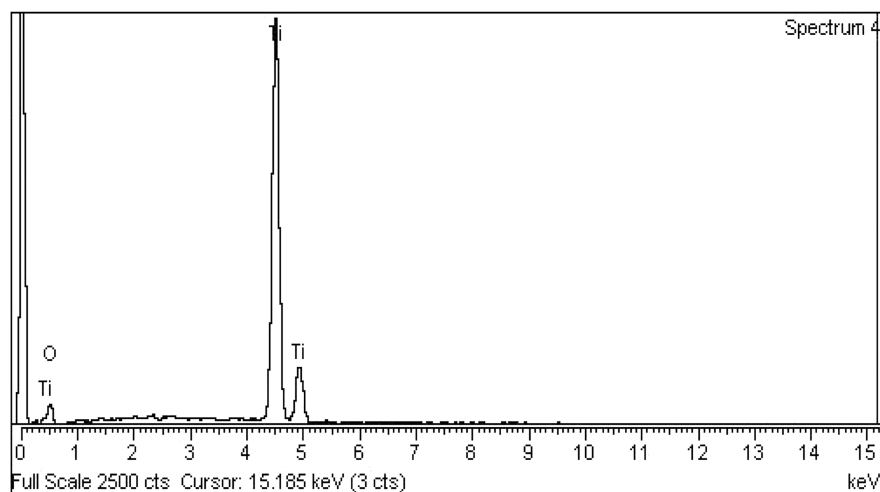


Figure 5. EDX analysis of TiO₂ NPs.

reduced particle size is inverse. As a result, smaller particles quickly penetrated toxic substances and the surfaces of cell samples, which triggered the decomposition process.³²

EDX Analysis of TiO₂ NPs. The purity of the synthesized TiO₂ NPs was confirmed by energy dispersive X-ray (EDX) analysis. A distinct signal was found in the elemental composition of synthetic TiO₂ NPs synthesized with plant extract from *Solanum surattense*. Figure 5 shows the strong absorption peak at 4–5 keV was due to the TiO₂ NPs. However, the strong signals are for titanium while the weaker signals are for oxygen, indicating the presence of TiO₂ in the sample. The result demonstrated that titanium and oxygen were present in titanium dioxide nanoparticles, and the lack of a peak indicates that a high degree of purity was present in naturally occurring nanoparticles.³³

Antiepileptic Activity. Effect of TiO₂ NPs on PTZ-Induced Epilepsy. A commonly known model of chemically induced seizures is produced using pentylenetetrazol (PTZ). Pentylene-tetrazol-induced seizures are categorized as a model of generalized seizure among all animal models of seizure and epilepsy to examine the effectiveness of TiO₂ NPs. Figure 6

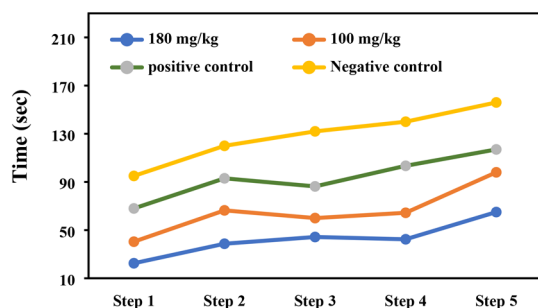


Figure 6. Effect of TiO₂ NPs on PTZ-induced epilepsy.

depicts the effects of the TiO₂ NP treatment on PTZ-induced epilepsy in rats. In this model, rats were pretreated with TiO₂ NPs (100 mg/kg and 180 mg/kg), phenytoin (25 mg/kg) for the positive control, and 2 mL/kg 10% v/v Tween 80 as the negative control. The results showed that the duration of different stages of convulsions induced by the PTZ model was drastically reduced by the treatment of TiO₂ NPs in contrast to control groups. The plant extracts are rich in many

phytochemicals, especially phenols and flavonoids, which are thought to exert antiepileptic effects by modulating channels. Hence, the synthesized TiO₂ NPs efficiently reduced the duration of seizures as compared to other test samples. The TiO₂ NPs at 180 mg/kg appeared to delay the onset of seizures (22.5 ± 0.13 , 38.7 ± 0.45 , 49.3 ± 0.40 , 42.4 ± 0.55 , and 65.0 ± 5.50 s) for each step, while the control groups shortened the duration of seizure in the range from 68.0 ± 1.96 to 117.0 ± 16.30 s, though the drug TiO₂ NPs prevents the seizures. It was demonstrated that the effectiveness of TiO₂ NPs depends on the concentration and works in a dose-dependent manner, whereas the concentrations of phenytoin are associated with the type of seizure control and toxicity. Some patients only require low phenytoin concentrations to attain complete seizure control, while others obtain benefit from concentrations in greater amounts without any adverse effects. This variability may be due to the seizure type, the severity of the underlying disorder, or genetic abnormalities. Therefore, the standard concentrations of phenytoin (25 mg/kg and 2 mL/kg, 10% v/v Tween 80) were used as the negative control and positive control, respectively. Similarly, 300 mg/kg *Silybum marianum* seed extract was used, which demonstrate the obvious stability against PTZ-induced convulsions (fatality, duration, and seizure frequency). Moreover, a 300 mg/kg dose of the extract was observed to be efficient in preventing oxidative stress in the brain of mice, leading to significantly higher antiepileptic activity.³⁴

Effect of TiO₂ NPs on MESE-Induced Epilepsy. The treatment-resistant epileptic patients were tested using the maximal electroshock seizure (MESE) model to demonstrate the effectiveness of antiepileptic medications against generalized and partial seizure epilepsy. The effect of TiO₂ NPs on MESE induced epilepsy treated rats led to significantly decreased seizure duration in the MESE model in comparison with phenytoin for the positive control and 2 mL/kg 10% v/v Tween 80 was used as negative control, as shown in Figure 7. The results revealed the time spent in each stage (clonus, extensor, and flexion) in the MESE model was significantly decreased by synthesized TiO₂ NPs as compared to control groups. Therefore, it was concluded that nonconvulsion epileptic seizure was observed 20.5 ± 0.14 , 16.8 ± 0.25 , and 15.3 ± 0.20 for flexion, extensor, and clonus at a 180 mg/kg dose concentration, respectively. The nonconvulsion epileptic seizure decreases as the concentration of TiO₂ NPs increases. Likewise,

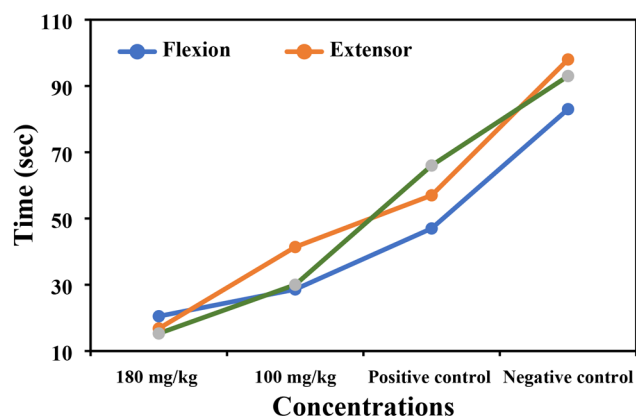


Figure 7. Effect of TiO₂ NPs on MESE-induced epilepsy in rats.

results were obtained by MESE was characterized by the appearance of clonus, extensor, and flexion. These stages were more pronounced in the negative control group and were substantially decreased in the treatment groups.^{24,35}

Biocompatibility Assessment. Cytotoxic Activity. The MTT assay was used to examine the cell viability of nanoparticles against THP-1 cells after overnight incubation. The cytotoxicity of TiO₂ NPs was evaluated after 8, 16, and 24 h, as showed in Figure 8. After 8 h of exposure, 88.4% of the cells

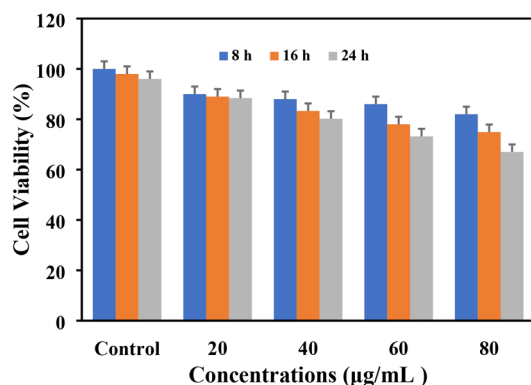


Figure 8. Concentration and time-dependent Cytotoxicity of TiO₂ NPs in cells determined using % MTT reduction.

were still viable at concentrations of 20 µg/mL of TiO₂ NPs (compared to 100% for the control). The reduction in cell viability was found to be approximately 80.2% after 24 h at a concentration of 40 µg/mL, which demonstrates that TiO₂ NPs were active toward THP-1 cells. Thus, the cell viabilities were approximately 73.2% and 67.0% as the concentration of nanoparticles increased to 60 and 80 µg/mL after 24 h, respectively. Hence, our data also demonstrate that no pronounced effect was acquired at lower concentrations with shorter time intervals; significant cytotoxicity was only detected after a 24 h time period at concentrations of 40, 60, and 80 µg/mL TiO₂ NP. In general, the cytotoxicity of TiO₂ NPs depends on the size, type of the surface coating, and crystal structure of the nanoparticles. Therefore, the small TiO₂ NPs have the potential to cross the cellular barriers and exhibit toxic effects through the generation of ROS in exposed cells.^{36,37} The TiO₂ NPs produce reactive oxygen species (ROS) that cause oxidative stress in cells and lead to the death of THP-1 cells.³⁸ It was

demonstrated that TiO₂ NPs increased the cytotoxicity of THP-1 cells in a dose-dependent manner.

CONCLUSION

It is concluded that the green synthesis of TiO₂ NPs was attained using the plant extract of *Solanum surattense*, which reduces the use of hazardous chemicals through a simple, inexpensive, and environmentally friendly process. FT-IR spectroscopy was used to analyze different functional groups and the interaction sites of macromolecules present in plant extract that act as reducing and capping agents for the synthesis of TiO₂ NPs. SEM confirmed the morphology of synthesized nanoparticles, whereas the crystalline nature and the particle size TiO₂ NPs were investigated by XRD analysis. The TiO₂ NPs showed desirable antiepileptic and cytotoxic activities. The antiepileptic activity of the synthesized nanoparticles was explored through maximal electroshock-induced epileptic (MESE) and pentylenetetrazol (PTZ) models. The synthesized nanoparticles significantly reduced the effects of the well-known PTZ and MESE models. Moreover, a higher cell viability was observed against THP-1 cell lines at a concentration of 80 µg/mL, which demonstrated that TiO₂ NPs showed significant cytotoxic activity.

ASSOCIATED CONTENT

Data Availability Statement

All the data generated and analyzed has already been incorporated into the study.

AUTHOR INFORMATION

Corresponding Authors

Fozia Fozia – Biochemistry Department, Khyber Medical University Institute of Medical Sciences, Kohat, Khyber Pakhtunkhwa 26000, Pakistan; orcid.org/0000-0002-4554-7427; Email: drfoziazeb@yahoo.com

Ijaz Ahmad – Department of Chemistry, Kohat University of Science and Technology, Kohat, Khyber Pakhtunkhwa 26000, Pakistan; Email: drijaz_chem@yahoo.com

Authors

Mohamed Mohany – Department of Pharmacology and Toxicology, College of Pharmacy, King Saud University, Riyadh 11451, Saudi Arabia

Ihsan Ullah – Department of Chemistry, Kohat University of Science and Technology, Kohat, Khyber Pakhtunkhwa 26000, Pakistan

Madeeha Aslam – Department of Chemistry, Kohat University of Science and Technology, Kohat, Khyber Pakhtunkhwa 26000, Pakistan

Majid Sharifi-Rad – Department of Range and Watershed Management, Faculty of Water and Soil, University of Zabol, Zabol 98613-35856, Iran

Salim S. Al-Rejaie – Department of Pharmacology and Toxicology, College of Pharmacy, King Saud University, Riyadh 11451, Saudi Arabia

Nouf S. S. Zaghloul – Bristol Centre for Functional Nanomaterials, HH Wills Physics Laboratory, University of Bristol, Bristol BS8 1FD, U.K.

Shakeel Ahmad – Department of Chemistry, Kohat University of Science and Technology, Kohat, Khyber Pakhtunkhwa 26000, Pakistan

Mourad A. M. Aboul-Soud – Department of Clinical Laboratory Sciences, College of Applied Medical Sciences, King Saud University, Riyadh 11433, Saudi Arabia

Complete contact information is available at:
<https://pubs.acs.org/10.1021/acsomega.3c00858>

Author Contributions

Conceptualization: F.F. and I.A.. Data curation: M.A. Formal analysis: F.F. Funding acquisition: M.M. Investigation: I.U., F.F., and S.A. Methodology: M.M. and I.U. Project administration: I.A. Resources: M.M. and I.A. Supervision: I.A. Visualization: M.S.-R. Writing, original draft: M.M., I.U., and M.A. Writing, review and editing: F.F., I.A., M.S.-R., S.A.-R., N.S.S.Z., and M.A.M.A.-S.

Funding

This research was funded through the Researchers Supporting Project (RSPD2023R758), King Saud University, Riyadh, Saudi Arabia.

Notes

The authors declare no competing financial interest.

REFERENCES

- (1) Moura, D.; Souza, M. T.; Liverani, L.; Rella, G.; Luz, G. M.; Mano, J. F.; Boccaccini, A. R. Development of a bioactive glass-polymer composite for wound healing applications. *Mater. Sci. Eng.* **2017**, *76*, 224–232.
- (2) Khan, I.; Saeed, K.; Khan, I. Nanoparticles: Properties, applications and toxicities. *Arab. J. Chem.* **2019**, *12* (7), 908–931.
- (3) Nabi, G.; Raza, W.; Tahir, M. B. Green synthesis of TiO₂ nanoparticle using cinnamon powder extract and the study of optical properties. *J. Inorg. Organomet. Polym. Mater.* **2020**, *30*, 1425–1429.
- (4) Govindasamy, G.; Murugasen, P.; Sagadevan, S. Investigations on the synthesis, optical and electrical properties of TiO₂ thin films by chemical bath deposition (CBD) method. *Mater. Res.* **2016**, *19*, 413–419.
- (5) Bedikyan, L.; Zakhariyev, S.; Zakhariyeva, M. Titanium dioxide thin films: preparation and optical properties. *J. Chem. Technol. Metall.* **2013**, *48* (6), 555–558.
- (6) Chen, H.; Liang, J.; Dong, K.; Yue, L.; Li, T.; Luo, Y.; Feng, Z.; Li, N.; Hamdy, M. S.; Alshehri, A. A.; Wang, Y.; et al. Ambient electrochemical N₂-to-NH₃ conversion catalyzed by TiO₂ decorated juncus effusus-derived carbon microtubes. *Inorg. Chem. Front.* **2022**, *9* (7), 1514–1519.
- (7) Wang, H.; Zhao, D.; Liu, C.; Fan, X.; Li, Z.; Luo, Y.; Zheng, D.; Sun, S.; Chen, J.; Zhang, J.; Liu, Y.; et al. FeS₂@ TiO₂ nanobelt array enabled high-efficiency electrocatalytic nitrate reduction to ammonia. *J. Mater. Chem. A* **2022**, *10* (46), 24462–24467.
- (8) Ren, W.; Yan, Y.; Zeng, L.; Shi, Z.; Gong, A.; Schaaf, P.; Wang, D.; Zhao, J.; Zou, B.; Yu, H.; Chen, G.; et al. A near infrared light triggered hydrogenated black TiO₂ for cancer photothermal therapy. *Adv. Health. Mater.* **2015**, *4* (10), 1526–1536.
- (9) Sargazi, S.; ER, S.; Sacide Gelen, S.; Rahdar, A.; Bilal, M.; Arshad, R.; Ajalli, N.; Farhan Ali Khan, M.; Pandey, S. Application of titanium dioxide nanoparticles in photothermal and photodynamic therapy of cancer: An updated and comprehensive review. *J. Drug Delivery Sci. Technol.* **2022**, *75*, 103605.
- (10) Anbumani, D.; vizhi Dhandapani, K.; Manoharan, J.; Babujanathanam, R.; Bashir, A. K. H.; Muthusamy, K.; Alfarhan, A.; Kanimozhi, K. Green synthesis and antimicrobial efficacy of titanium dioxide nanoparticles using *Luffa acutangula* leaf extract. *J. King Saud Univ. Sci.* **2022**, *34* (3), 101896.
- (11) Li, Y.; Xia, Y.; Liu, K.; Ye, K.; Wang, Q.; Zhang, S.; Huang, Y.; Liu, H. Constructing Fe-MOF-derived Z-scheme photocatalysts with enhanced charge transport: nanointerface and carbon sheath synergistic effect. *ACS Appl. Mater. Interfaces* **2020**, *12* (22), 25494–25502.
- (12) Ouyang, L.; He, X.; Sun, Y.; Zhang, L.; Zhao, D.; Sun, S.; Luo, Y.; Zheng, D.; Asiri, A. M.; Liu, Q.; Zhao, J.; et al. RuO₂ nanoparticle-decorated TiO₂ nanobelt array as a highly efficient electrocatalyst for the hydrogen evolution reaction at all pH values. *Inorg. Chem. Front.* **2022**, *9* (24), 6602–6607.
- (13) Taheriniya, S.; Behboodi, Z. Comparing green chemical methods and chemical methods for the synthesis of titanium dioxide nanoparticles. *Int. J. Pharm. Sci. Res.* **2016**, *7* (12), 4927–4932.
- (14) Wu, F.; Zhou, Z.; Hicks, A. L. Life cycle impact of titanium dioxide nanoparticle synthesis through physical, chemical, and biological routes. *Environ. Sci. Technol.* **2019**, *53* (8), 4078–4087.
- (15) Fan, X.; He, X.; Ji, X.; Zhang, L.; Li, J.; Hu, L.; Li, X.; Sun, S.; Zheng, D.; Luo, Y.; Wang, Y.; et al. High-efficiency electrosynthesis of ammonia with selective reduction of nitrite over Ag nanoparticles-decorated TiO₂ nanoribbon array. *Inorg. Chem. Front.* **2023**, *10*, 1431–1435.
- (16) Ansari, A.; Siddiqui, V. U.; Rehman, W. U.; Akram, M.; Siddiqui, W. A.; Alosaimi, A. M.; Hussein, M. A.; Rafatullah, M. Green synthesis of TiO₂ nanoparticles using *Acorus calamus* leaf extract and evaluating its photocatalytic and in vitro antimicrobial activity. *Catalysts* **2022**, *12* (2), 181.
- (17) Al-Hamoud, K.; Shaik, M. R.; Khan, M.; Alkhatlan, H. Z.; Adil, S. F.; Kuniyil, M.; Assal, M. E.; Al-Warthan, A.; Siddiqui, M. R. H.; Tahir, M. N.; Khan, S. T.; et al. *Pulicaria undulata* extract-mediated eco-friendly preparation of TiO₂ nanoparticles for photocatalytic degradation of methylene blue and methyl Orange. *ACS Omega* **2022**, *7* (6), 4812–4820.
- (18) Giourou, E.; Stavropoulou-Deli, A.; Giannakopoulou, A.; Kostopoulos, G. K.; Koutroumanidis, M. Introduction to epilepsy and related brain disorders. *Cyberphysical Systems for Epilepsy and Related Brain Disorders: Multi-parametric Monitoring and Analysis for Diagnosis and Optimal Disease Management* **2015**, 11–38.
- (19) Bhat, J. U.; Nizami, Q.; Aslam, M.; Asiaf, A.; Ahmad, S. T.; Parray, S. A. Antiepileptic activity of the whole plant extract of *Melissa officinalis* in swiss albino mice. *Int. J. Pharm. Sci. Res.* **2012**, *3* (3), 886–889.
- (20) Shaikh, M. F.; Sancheti, J.; Sathaye, S. Phytochemical and pharmacological investigations of *Eclipta alba* (Linn.) Hassak leaves for antiepileptic activity. *Int. J. Pharm. Pharm. Sci.* **2012**, *4* (Suppl 4), 319–323.
- (21) Sahar, A.; Aftab, K.; Chaudhry, A. H.; Malik, T. A. Phytochemistry and biological importance of *Solanum surattense*. *World Appl. Sci. J.* **2018**, *36* (3), 529–536.
- (22) Tekuri, S. K.; Pasupuleti, S. K.; Konidala, K. K.; Amuru, S. R.; Bassaiahgari, P.; Pabbaraju, N. Phytochemical and pharmacological activities of *Solanum surattense* Burm. f.—A review. *J. Appl. Pharm. Sci.* **2019**, *9* (3), 126–136.
- (23) Santhoshkumar, T.; Rahuman, A. A.; Jayaseelan, C.; Rajakumar, G.; Marimuthu, S.; Kirthi, A. V.; Velayutham, K.; Thomas, J.; Venkatesan, J.; Kim, S. K. Green synthesis of titanium dioxide nanoparticles using *Psidium guajava* extract and its antibacterial and antioxidant properties. *Asian Pac. J. Trop. Med.* **2014**, *7* (12), 968–976.
- (24) Uddin, I.; Kalyani, D.; Tejasri, N.; Mounika, A.; Sowndarya, A.; Anitha, J.; Hussain, A. Green Synthesis and Characterization of Silver Nanoparticles using *Glycine Max* L. Seed Extract and their Antiepileptic Activity in Rats. *Int. J. Pharm. Sci. Nanotechnol. (IJPSN)* **2017**, *10* (6), 3909–3914.
- (25) Madhubala, V.; Pugazhendhi, A.; Thirunavukarasu, K. Cytotoxic and immunomodulatory effects of the low concentration of titanium dioxide nanoparticles (TiO₂ NPs) on human cell lines—An in vitro study. *Process Biochem.* **2019**, *86*, 186–195.
- (26) Rajakumar, G.; Rahuman, A. A.; Roopan, S. M.; Chung, I. M.; Anbarasan, K.; Karthikeyan, V. Efficacy of larvicidal activity of green synthesized titanium dioxide nanoparticles using *Mangifera indica* extract against blood-feeding parasites. *Parasitol. Res.* **2015**, *114*, 571–581.
- (27) Srinivasan, M.; Venkatesan, M.; Arumugam, V.; Natesan, G.; Saravanan, N.; Murugesan, S.; Ramachandran, S.; Ayyasamy, R.; Pugazhendhi, A. Green synthesis and characterization of titanium dioxide nanoparticles (TiO₂ NPs) using *Sesbania grandiflora* and evaluation of toxicity in zebrafish embryos. *Process Biochem.* **2019**, *80*, 197–202.
- (28) Rajakumar, G.; Rahuman, A. A.; Priyamvada, B.; Khanna, V. G.; Kumar, D. K.; Sujin, P. J. *Eclipta prostrata* leaf aqueous extract mediated

synthesis of titanium dioxide nanoparticles. *Mater. Lett.* **2012**, *68*, 115–117.

(29) Subhapiya, S.; Gomathipriya, P. Green synthesis of titanium dioxide (TiO₂) nanoparticles by *Trigonella foenum-graecum* extract and its antimicrobial properties. *Microb. pathog.* **2018**, *116*, 215–220.

(30) Gandhi, P. R.; Jayaseelan, C.; Kamaraj, C.; Rajasree, S. R.; Mary, R. R. In vitro antimalarial activity of synthesized TiO₂ nanoparticles using *Momordica charantia* leaf extract against *Plasmodium falciparum*. *J. Appl. Biomed.* **2018**, *16* (4), 378–386.

(31) Rajakumar, G.; Rahuman, A. A.; Roopan, S. M.; Khanna, V. G.; Elango, G.; Kamaraj, C.; Zahir, A. A.; Velayutham, K. Fungus-mediated biosynthesis and characterization of TiO₂ nanoparticles and their activity against pathogenic bacteria. *Spectrochim. Acta Part A Mol. Biomol. Spectrosc.* **2012**, *91*, 23–29.

(32) Chatterjee, A.; Ajantha, M.; Talekar, A.; Revathy, N.; Abraham, J. Biosynthesis, antimicrobial and cytotoxic effects of titanium dioxide nanoparticles using *Vigna unguiculata* seeds. *Int. J. Pharm. Phytochem. Res.* **2017**, *9* (1), 95–99.

(33) Aravind, M.; Amalanathan, M.; Mary, M. S. M. Synthesis of TiO₂ nanoparticles by chemical and green synthesis methods and their multifaceted properties. *SN Appl. Sci.* **2021**, *3*, 409.

(34) Waqar, H.; Khan, H. M.; Anjum, A. A. Antiepileptic potential of *Silybum marianum* seeds in pentylenetetrazol-induced kindled mice. *Bangladesh J. Pharmacol.* **2016**, *11* (3), 603–609.

(35) Rajput, M. A.; Khan, R. A.; Assad, T. Anti-epileptic activity of *Nelumbo nucifera* fruit. *Metab. Brain Dis.* **2017**, *32*, 1883–1887.

(36) Gato, M. A.; Naseem, S.; Arfat, M. Y.; Mahmood Dar, A.; Qasim, K.; Zubair, S. Physicochemical properties of nanomaterials: implication in associated toxic manifestations. *BioMed. Res. Int.* **2014**, *2014*, 498420.

(37) Jin, C.; Tang, Y.; Yang, F. G.; Li, X. L.; Xu, S.; Fan, X. Y.; Huang, Y. Y.; Yang, Y. J. Cellular toxicity of TiO₂ nanoparticles in anatase and rutile crystal phase. *Biol. Trace Elem. Res.* **2011**, *141*, 3–15.

(38) Limbach, L. K.; Wick, P.; Manser, P.; Grass, R. N.; Bruinink, A.; Stark, W. J. Exposure of engineered nanoparticles to human lung epithelial cells: influence of chemical composition and catalytic activity on oxidative stress. *Environ. Sci. Technol.* **2007**, *41* (11), 4158–4163.